



Published in final edited form as:

*Nat Neurosci.* 2017 July ; 20(7): 1023–1032. doi:10.1038/nn.4564.

## A FluoroNissl dye identifies pericytes as distinct vascular mural cells during *in vivo* brain imaging

Eyiyemisi C. Damisah<sup>1,2,4</sup>, Robert A. Hill<sup>1,3,4</sup>, Lei Tong<sup>1,3</sup>, Katie N. Murray<sup>1,3</sup>, and Jaime Grutzendler<sup>1,3,#</sup>

<sup>1</sup>Department of Neurology, Yale School of Medicine, New Haven, CT 06511, USA

<sup>2</sup>Department of Neurosurgery, Yale School of Medicine, New Haven, CT 06511, USA

<sup>3</sup>Department of Neuroscience, Yale School of Medicine, New Haven, CT 06510, USA

### Abstract

Pericytes and smooth muscle cells are integral components of the brain microvasculature. However, no techniques exist to unambiguously identify these cell types, greatly limiting their investigation *in vivo*. Here we show that a fluorescent Nissl dye (NeuroTrace 500/525) labels brain pericytes with exquisite specificity allowing high-resolution optical imaging in the live mouse. We demonstrate that capillary pericytes are a population of mural cells with distinct morphological, molecular, and functional features that do not overlap with pre-capillary or arteriolar smooth-muscle actin-expressing cells. The remarkable specificity for dye uptake suggests that pericytes have molecular transport mechanisms not present in other brain cells. We demonstrate feasibility for longitudinal pericyte imaging during microvascular development and aging and in models of brain ischemia and Alzheimer's disease. The ability to easily label pericytes in any mouse model opens the possibility of a broad range of investigations of mural cells in vascular development, neurovascular coupling and neuropathology.

---

Microvascular smooth muscle cells (SMCs) and pericytes play fundamental roles in the development and maintenance of the brain's vascular network and the blood brain barrier (BBB), signaling within the neurovascular unit, and modulation of micro-regional cerebral blood flow (CBF)<sup>1–7</sup> and have been implicated in a large number of neuropathological processes<sup>2, 8, 9</sup>. However, precise investigation has been greatly limited by the inability to unambiguously differentiate between the different subtypes of vascular mural cells due to

---

Users may view, print, copy, and download text and data-mine the content in such documents, for the purposes of academic research, subject always to the full Conditions of use: [http://www.nature.com/authors/editorial\\_policies/license.html#terms](http://www.nature.com/authors/editorial_policies/license.html#terms)

#corresponding author [jaimе.grutzendler@yale.edu](mailto:jaimе.grutzendler@yale.edu).

<sup>4</sup>These authors contributed equally to this work

### DATA AVAILABILITY

The data that support the findings of this study are available from the corresponding author upon reasonable request.

### AUTHOR CONTRIBUTIONS

E.C.D., R.A.H., and J.G. made the initial observation and designed all the experiments. E.C.D. and R.A.H. performed the morphological, developmental, and functional characterization of dye labeled cells. L.T. conducted Alzheimer's mouse model characterization and prepared tissue for electron microscopy. K.N.M. performed fixed tissue quantification and surgeries for carotid occlusion experiments. R.A.H. and J.G. wrote the manuscript with input from all authors. J.G. supervised the study.

### COMPETING FINANCIAL INTERESTS

The authors declare no competing financial interests.

the fact that they share many protein markers and have heterogeneous morphology with ambiguous boundaries at the transition between precapillary arterioles and capillaries<sup>7, 10–13</sup>. Thus despite the fact that these cells can be broadly grouped into two distinct categories: one type with ring-like morphology and expression of the contractile protein  $\alpha$ -smooth muscle actin ( $\alpha$ -SMA) and another type with long and thin processes and no  $\alpha$ -SMA, there is still considerable debate about the extent to which these are different cell types with different functions<sup>2, 7, 10–17</sup>. Development of new tools that allow unambiguous separation of these cells during *in vivo* imaging would greatly enhance the ability to study the physiology and pathology of the neurovascular unit.

We have discovered that a commercially available small molecule fluorescent dye, a FluoroNissl Green<sup>18</sup> derivative called NeuroTrace 500/525 exclusively and efficiently labels capillary pericytes in the live brain upon topical application or intracortical microinjection. Using transgenic reporter mice and dynamic imaging of spontaneous vasomotility in awake mice we demonstrate that this dye specifically labels non-contractile vascular mural cells embedded within two layers of basal lamina with long thin processes spanning multiple vessel branches and with no  $\alpha$ -SMA expression. In contrast, adjacent contractile  $\alpha$ -SMA-expressing vascular mural cells with ring-like morphology do not label with this dye, strongly suggesting that these cells constitute distinct and non-overlapping populations.

We demonstrate the use of this dye for dynamic imaging in models of cerebral ischemia, aging, and Alzheimer's disease and during early postnatal brain microvascular development. Thus, we provide the first method for exclusive identification and *in vivo* imaging of capillary pericytes in the healthy and diseased brain. This method can be applied immediately without the need for transgenic reporter mice and is likely to have broad applications in many fields of research including development and pathology of the neurovascular unit, neurovascular coupling and neurodegeneration. In addition, the robust and selective dye labeling may allow specific pericyte isolation for gene expression and proteomic studies. It also raises interesting questions regarding the possible expression of unique molecular transport mechanisms in pericytes that explain their selective dye uptake.

## RESULTS

### Specific and robust dye labeling of capillary pericytes in the live mouse brain

As we were screening various dyes for differential properties of cell labeling in the live mouse brain, we noticed that a fluorescent Nissl<sup>18</sup> derivative with affinity for Nissl bodies (NeuroTrace 500/525 but not other NeuroTrace variants), commonly used to label neurons in fixed tissues, had very unique properties when applied to the mouse brain *in vivo*. Instead of neuronal labeling as expected, topical application of this dye through a cranial window led to labeling of a distinct population of cells lining cerebral blood vessels up to 400 $\mu$ m deep into the cortex (Fig. 1a and Supplementary Video 1). Labeled cells lined the smallest cerebral vessels and had the morphology of capillary pericytes<sup>7, 13</sup> with multiple slender processes extending longitudinally and spanning several vessel branches (Fig. 1). Dye labeling was very bright and concentrated in cell soma as well as throughout the processes where it displayed a punctate pattern (Fig. 1a–b). Pericyte labeling remained strong over 2–3 days and by day 4 it had mostly disappeared. Importantly, we did not observe any signs of

cellular toxicity as a result of the dye administration and subsequent imaging as evidenced by the lack of changes in cellular morphology over intervals up to 3 days.

Surprisingly, no other parenchymal brain cell type was labeled at all (some meningeal and perivascular macrophages at the site of topical dye application were transiently labeled). Co-labeling with the fluorescent dye Sulforhodamine 101 (SR101) which labels astrocytes and oligodendrocytes<sup>19, 20</sup> showed no co-localization, confirming that neither of these cell types is labeled by NeuroTrace (Fig. 1b). To precisely determine the identity of the labeled cells we applied the dye to the cortex of transgenic mice with fluorescent protein labeling of all vascular mural cells (*PDGFR $\beta$ cre:Tomato*)<sup>13, 21</sup> which have 99 $\pm$ 1% co-localization between PDGFR $\beta$  antibody stained cells and genetically labeled Tomato expressing cells (Supplementary Fig. 1, n=3 mice, 948 PDGFR $\beta$  + cells / 957 Tomato+ cells). NeuroTrace dye labeling co-localized specifically with fusiform capillary pericytes (99 $\pm$ 0.1% of all NeuroTrace labeled cells were co-labeled with Tomato *in vivo*, n=3 mice, 305 NeuroTrace+ Tomato+ cells / 307 NeuroTrace+ cells) and not with ring-like precapillary or arteriolar SMCs (Fig. 2). Additionally we confirmed that NeuroTrace was exclusive to vascular pericytes in a separate commonly used transgenic mouse line with vascular mural cells and cells of the oligodendrocyte lineage labeling (*NG2cre:Tomato*)<sup>7, 13, 22, 23</sup>. Again, dye labeling was found specifically in fusiform capillary pericytes and not in ring-like precapillary or arteriolar SMCs nor in NG2-glia or oligodendrocytes (Fig. 3). Discrete transition points from dye-negative SMCs to dye-labeled pericytes were clearly observed (Fig. 3a). In the *NG2cre* mouse line all pericytes are not labeled due to incomplete Cre recombination<sup>13, 22</sup>, in contrast to NeuroTrace which provided complete labeling of all pericytes within the dye-labeled brain region (Fig. 3c–d).

To further confirm that the NeuroTrace labeled cells were indeed pericytes embedded within the basal lamina<sup>2</sup> we performed high resolution confocal imaging with deconvolution, of collagen IV basal lamina antibody staining surrounding cells labeled with NeuroTrace and *PDGFR $\beta$ cre:Tomato* (Fig. 4, Supplementary Fig. 2). This approach allowed direct visualization of the two layers of the basal lamina with molecular specificity (Fig. 4, Supplementary Fig. 2). All *PDGFR $\beta$ cre:Tomato* cells with capillary pericyte morphology were imbedded within the collagen IV labeled basal lamina (Fig. 4a–b). NeuroTrace dye diffuses out of pericytes that are labeled through *in vivo* cortical dye application during immunostaining. Thus, we had to perform sequential imaging of the same cell before and after immunostaining to directly detect dual basal lamina surrounding cells that had previously been labeled with NeuroTrace. All cells that were labeled with NeuroTrace and sequentially imaged in this manner displayed robust two-layer collagen IV labeled basal lamina (Fig. 4c, Supplementary Fig. 2, n=11 cells). To provide additional evidence of this cellular localization we attempted to photooxidize NeuroTrace for diaminobenzidine (DAB) detection at the ultrastructural level (Fig. 4d). Photooxidation is known to have heterogeneous success rates for different dyes<sup>24, 25</sup> and we had some limited success (Fig. 4d) at detecting the DAB signal in pericytes using transmission electron microscopy. Reasons for this could be due to the dye likely being a poor photooxidizer as has been shown for other dyes<sup>24, 25</sup>. Nonetheless, this combination of approaches allowed us to conclusively demonstrate that NeuroTrace-labeled cells are indeed embedded within two

layers of basal lamina, further confirming that they are indeed capillary pericytes (Fig. 4, Supplementary Fig. 2)

There are two potential routes for the NeuroTrace dye to enter the brain: 1) directly through the glia limitans into the interstitial space<sup>26</sup> or 2) diffusion through the perivascular Virchow-Robbins space. The second route has the potential to result in predominant pericyte labeling given their perivascular location. Thus, to bypass these barriers and test if the dye specifically labels pericytes regardless of entry route, we directly microinjected NeuroTrace into the parenchyma through a pulled glass capillary (Supplementary Fig. 3a). Two-photon time-lapse imaging during dye injection revealed exclusive pericyte labeling within minutes with no labeling of other cell types (Supplementary Fig. 3a–c, Supplementary Video 2). Thus, the specificity of labeling is likely due to an intrinsic property of capillary pericytes that is absent from any other brain cell, including the immediately adjacent perivascular SMCs. This specificity, combined with the robust labeling brightness and persistence over days makes the use of this dye to our knowledge, the first method to unambiguously image and distinguish capillary pericytes from all other brain cells *in vivo*.

### NeuroTrace-labeled pericytes do not exhibit spontaneous contractility

Neurovascular coupling is a critical brain homeostatic function that is controlled by complex interactions between cells of the neurovascular unit<sup>9</sup>. There is ongoing debate as to which subsets of mural cells are ultimately responsible for vascular dilation and contraction and whether there are subsets of capillary pericytes capable of mediating vasomotility<sup>7, 10, 13</sup>. Resolving this controversy is critical for our understanding of neurovascular coupling and blood flow control. To determine if NeuroTrace-labeled pericytes were present on vessels which exhibit active vasomotility we performed *in vivo* imaging in transgenic mice with mCherry labeling of smooth muscle actin expressing cells SMCs (*SMA-mCherry*)<sup>7, 27</sup> (Fig. 5). NeuroTrace exclusively labeled mural cells that did not express mCherry on vessels ranging in diameter from 2.3–13.7  $\mu\text{m}$  (average =  $5.3 \pm 2.2 \mu\text{m}$ , 104 vessel locations from n=5 mice) (Fig. 5c). *SMA-mCherry* covered vessels that were not labeled with NeuroTrace had a range of diameters from 2.9–29.9  $\mu\text{m}$  (average =  $9.6 \pm 4.7 \mu\text{m}$ , 115 vessel locations from n=5 mice) (Fig. 5c). Consistent with *NG2cre:Tomato* mice (Fig. 3), NeuroTrace was able to precisely highlight transition points from completely un-labeled SMCs to strongly labeled pericytes (Fig. 5b). Furthermore, consistent with *SMA-mCherry* labeling, the arteriolar specific dye 633-hydrazide<sup>28</sup> exclusively labeled vessels that were not labeled with NeuroTrace (Fig. 5d), providing additional evidence of the existence of two distinct populations of mural cells, SMA expressing SMCs on arterioles and NeuroTrace-labeled pericytes on capillaries.

In order to determine if these two populations of cells exhibited different functions we performed *in vivo* time lapse imaging of spontaneous vasomotion in awake and anesthetized mice. As was recently shown<sup>7, 14</sup>, spontaneous vasomotility was found exclusively in SMC but not pericyte covered vessels based on a measure that accounts for amplitude, frequency, and duration of diameter changes, termed vasomotility index<sup>7</sup> (see methods) (Fig. 6). Thus, NeuroTrace specifically labels non-contractile capillary pericytes and does not label contractile pre-capillary and arteriolar  $\alpha$ SMA-expressing mural cells. Therefore,

NeuroTrace provides a novel method for *in vivo* investigations of differential mural cell physiology during neurovascular coupling and potentially during pathological processes.

### **Intravital imaging of pericytes during development and aging, in cerebral ischemia, and Alzheimer's models**

A major challenge for determination of capillary pericyte function in aging and neuropathological conditions has been the lack of methods for precise identification and visualization during dynamic *in vivo* experimentation. Therefore, we explored whether NeuroTrace labeling could be used in a range of conditions where pericyte dysfunction has been implicated. First, NeuroTrace labeling in early postnatal stages, adult, and aged 29 month old wildtype mice revealed brightly labeled pericytes with no significant differences in dye labeling quality or distribution between P10, P60 and P870 mice (Fig. 7a–b) (P10:  $3388 \pm 769$  cells/mm<sup>3</sup>, P60:  $2860 \pm 166$  cells/mm<sup>3</sup>, P870:  $3245 \pm 317$  cells/mm<sup>3</sup>, n=3 mice per group, two-way ANOVA, Bonferroni posttest). In addition to quantification of cell density we also observed dye labeled pericyte cell bodies and processes not associated with perfused vessels (Figure 7c–d). These cells were more prevalent in P10 mice compared to P60 and P870 likely due to pericyte association with non-perfused vascular sprouts<sup>29–31</sup> (P10:  $173 \pm 91$  cells/mm<sup>3</sup>, P60:  $24 \pm 28$  cells/mm<sup>3</sup>, P870:  $28 \pm 36$  cells/mm<sup>3</sup>, n=3 mice per group, two-way ANOVA, Bonferroni posttest). Interestingly however pericytes bridging regions with no evident perfused vessels were also found in adult and aged mice when the majority of vascular structural plasticity has ended (Fig. 7d–e) suggesting potential signaling functions of these bridging cells and/or permanent remnants of developmental vascular pruning. Thus, NeuroTrace can be used for pericyte labeling to determine *in vivo* cell-cell interactions during development of the neurovascular unit and to test age-related mural cell associated vascular dysfunction in any wildtype or transgenic mouse model.

Next, we visualized pericytes in a model of transient ischemia via reversible bilateral common carotid artery occlusion (Supplementary Fig. 4a). This model, which has been previously characterized, allows dynamic imaging during the initial stages of ischemia. This is a time when cortical spreading depolarization, a known modulator of SMC contractility is highly prevalent, and early changes in vascular and neuronal pathology occur<sup>32</sup>. Five minutes of bilateral carotid occlusion resulted in marked reduction in CBF and resulted in reversible collapse/constriction of vessels specifically covered by SMA-expressing SMCs ( $-56 \pm 14.7\%$  change in diameter, 23 vessel locations from n=3 mice) (Supplementary Fig. 4b–e). In contrast, NeuroTrace labeled pericyte covered capillaries displayed decreased or stalled blood flow but did not exhibit significant changes in diameter ( $-3 \pm 1.4\%$  change in diameter, 28 vessel locations from n=3 mice) (Supplementary Fig. 4b–e). Thus, it appears that only  $\alpha$ SMA positive but not NeuroTrace labeled cells significantly contract during transient ischemia. This dye could thus be used to identify pericytes for a variety of studies during ischemic pathology.

Finally, as smooth muscle cells and pericytes have been implicated in the pathogenesis of Alzheimer's disease (AD)<sup>8,9</sup>, we visualized pericytes in a mouse model of AD (*5xFAD*). Amyloid plaques and cerebral amyloid angiopathy (CAA) were labeled with the amyloid binding dye Thioflavin S (Fig. 8a–b). Consistent with our finding in aged wildtype mice,

NeuroTrace labeling in *5xFAD* mice was similar to wildtype aged matched controls (Fig. 8c) (wildtype:  $2999 \pm 254$  cells/mm<sup>3</sup>, *5xFAD*:  $2982 \pm 162$  cells/mm<sup>3</sup>, n=3 mice per group, p=0.947, t-test). Furthermore, NeuroTrace labeling was not detected on vessels which exhibited CAA (Fig. 8a–b) suggesting that overt amyloid aggregation may be exclusive to  $\alpha$ SMC-covered arterioles in these mice.

## DISCUSSION

Current approaches for pericyte identification in live animals rely on transgenic promoter expression based on the NG2 chondroitin sulfate proteoglycan or the beta receptor for platelet-derived growth factor (PDGFR $\beta$ )<sup>2, 7, 10, 13, 14</sup>. However, both of these markers label other cell types and there are no known exclusive genetic markers of pericytes, prohibiting their unambiguous separation from other vascular mural cells. Even currently available dual-reporter triple transgenic mice cannot exclusively label pericytes<sup>7</sup> thus the identification of a capillary pericyte specific marker is crucial for future studies. To our knowledge NeuroTrace labeling provides the first method for unambiguous *in vivo* identification of brain capillary pericytes separate from all other brain cells. NeuroTrace is easy to utilize during intravital imaging, it robustly and brightly labels capillary pericytes embedded within the vascular basal lamina and can be used for repeated imaging of these cells without acute evidence of toxicity. This method can now be implemented in numerous *in vivo* studies for broad interrogation of pericyte function throughout development into advanced aging and numerous models of brain pathology.

NeuroTrace exclusively labels capillary pericytes, which are cells with long processes that do not fully wrap around vessels, in contrast to immediately upstream precapillary and arteriolar ring-like mural cells. The specific nature of dye labeling to capillary pericytes combined with the fact that these cells have a unique morphology, do not express  $\alpha$ SMA and are not contractile, provides a strong line of evidence that pericytes are a discrete cell population that is distinct from immediately adjacent SMCs and that there are no transitional precapillary cells with hybrid properties. Furthermore, the exclusivity of dye uptake suggests a distinct molecular mechanism unique to brain capillary pericytes opening the possibility of future specific molecular targeting of pericytes for therapeutic purposes.

The precise role of capillary pericytes in neurovascular coupling is debated<sup>7, 10, 11, 14</sup>. Under anesthetized and awake conditions, we found no evidence of spontaneous changes in vessel diameter on vessels covered by NeuroTrace labeled pericytes. This was in contrast to immediately upstream vessels covered by  $\alpha$ -SMA expressing SMCs which exhibited robust spontaneous changes in diameter. These data provide additional independent evidence that these two populations of mural cells are indeed functionally, molecularly, and morphologically distinct with clear delineations at the transition point from contractile  $\alpha$ -SMA expressing SMC to non-contractile pericytes. Our findings are consistent with previous studies showing no significant changes in vessel diameter at the capillary level after sensory stimulation<sup>7, 11, 14, 33</sup>. These findings do not exclude a signaling role for pericytes in neurovascular coupling as the dynamic calcium fluctuations and gap junction coupling between these cells and others within the neurovascular unit suggest unique cell-to-cell signaling mechanisms under various situations<sup>7, 34–36</sup>. NeuroTrace now allows investigation

of the roles of these cells in the intact *in vivo* environment with fundamental implications for understanding the cellular mechanisms of CBF control.

Pericyte dysfunction has been implicated in several neuropathological states including brain ischemia and Alzheimer's disease<sup>8–10, 12, 37</sup>. Importantly, the inability to precisely identify pericytes in previous studies has limited the *in vivo* investigation of distinct contributions of different mural cell types to these diseases. The differences in our results compared to previous studies regarding pericyte changes, in aging and AD models are unclear. However, one possibility is that previous studies have generally pooled both SMCs and pericytes in their quantifications. Given the known presence of amyloid accumulation in arterioles, SMCs might be more vulnerable to age related changes than capillary pericytes.

NeuroTrace labeling now provides a rapidly adoptable method to exclusively label capillary pericytes in numerous aged wildtype and transgenic mouse models and potentially in other species. This tool will significantly facilitate future investigations of pericyte contributions to normal brain function and pathology.

## ONLINE METHODS

### Animals

All animal procedures were approved by the Institutional Animal Care and Use Committee (IACUC). Male and female mice aged P10-P870 housed in a 12hr light/dark cycle with 3–5 animals per cage were used. Animals were assigned randomly to groups and no animals were excluded from analysis. The following transgenic lines were used for visualization of defined cell populations: wildtype C57BL/6, NG2Cre<sup>22</sup> (Jax#008533), tdTomato reporter Ai14<sup>38</sup> (Jax#007914), SMA-mCherry<sup>27</sup>, PDGFR $\beta$ cre<sup>21</sup>, and Alzheimer's mouse model 5xFAD<sup>39</sup>.

### Cranial window preparation and *in vivo* imaging

Mouse cranial windows were prepared as previously described<sup>40</sup>. Briefly animals were anesthetized via intraperitoneal injections of 100 mg/kg ketamine and 10 mg/kg xylazine. A 3–4mm craniotomy was prepared over the somatosensory cortex and the underlying dura was removed. After dye labeling (see below) a #0 cover glass was placed over the exposed area and sealed with dental cement. For all experiments except awake imaging mice were imaged while anesthetized with a mixture of ketamine and xylazine as stated above. For awake imaging experiments (Figure 6) mice were habituated to head fixation and imaged through an acute cranial window during quiet waking. For chronic *in vivo* imaging a nut was fixed to the skull and embedded within dental cement for repeated imaging, head immobilization, and window orientation. Cerebral vessels were visualized by intravenous injection of 70,000mw Texas Red dextran, 10,000mw Cascade Blue dextran, or Evans Blue. To visualize the endothelium *in vivo* we intravenously injected PECAM 647 conjugated antibody. *In vivo* images were acquired using a two-photon microscope (Prairie technologies) equipped with a mode-locked MaiTai two-photon laser (Spectra Physics) and 20x water immersion objective (Zeiss 1.0 NA). The two-photon laser was tuned to the following wavelengths for optimal excitation of particular fluorophores: 1000nm for

NeuroTrace 500/525, SMA-mCherry, Evans Blue, and Texas Red dextran. In some cases, an upright Leica SP5 confocal microscope with a 20x water immersion objective (1.0 NA, Leica) was used for optimal fluorophore excitation and emission separation. For confocal imaging the following wavelengths were used 405nm for Cascade Blue Dextran, 488nm for GFP, 561nm for mCherry, tdTomato, and Texas Red Dextran and 633nm for Evans Blue and PECAM-647.

### Fluorescent dye labeling

NeuroTrace 500/525 dye was either applied topically (1:25 dilution in PBS) to the cortical surface for five minutes and then thoroughly washed, or 300nL was injected into the brain using a pulled glass pipette attached to a Nanoject II (Drummond Scientific). For topical application bright labeling was evident 3 hours after labeling and remained for at least 48 hours. For amyloid labeling in *5xFAD* mice, Thioflavin S (0.002% in PBS) was applied topically to the cortical surface for 30 minutes then washed thoroughly with PBS.

### Bilateral common carotid artery occlusion

Acute brain ischemia was achieved by temporary bilateral occlusion of the common carotid arteries (CCA) as previously described<sup>32</sup>. Briefly animals were anesthetized and the common carotid arteries were dissected and exposed and suture loops were placed around each vessel. The animal's skin was stitched while allowing the suture loops to extend through the incision for access during in vivo imaging. Animals were imaged in vivo with a confocal microscope to allow sufficient three color fluorophore separation. Z-stack time-lapse sequences were acquired for 20 minutes and ischemia was induced by tightening the suture loops with a micromanipulator to transiently block blood perfusion for 5 minutes during the 20-minute time lapse-sequence (Supplementary Fig. 4).

### Tissue collection and immunohistochemistry

Mice were anesthetized and perfused with 4% paraformaldehyde and post-fixed overnight at 4°C. 50µm thick brain tissue sections were cut on a vibratome and processed for immunohistochemistry. Tissue sections were blocked in 1 X PBS containing 5% normal goat serum (NGS), 0.5% bovine serum albumin (BSA) and 0.3% Triton-X-100 at room temperature. All primary and secondary antibodies were diluted in 1 X PBS containing 0.5% BSA and 0.3% Triton-X-100. Tissue sections were incubated in primary antibodies overnight at 4°C and secondary antibodies for 4 hours at room temperature. The following primary antibodies were used: collagen IV<sup>41</sup> (abcam cat# AB19808; 1:250 dilution), PDGFRβ<sup>42</sup> (eBioscience cat# 14-1402-82; 1:200) and NG2<sup>22, 43</sup> (Millipore cat# MAB5384; 1:100). Antigen retrieval was performed for collagen IV staining by incubating slices at 85°C for 20 minutes in PBS prior to blocking. Images were captured on a Leica SP5 laser scanning confocal microscope.

For sequential imaging of NeuroTrace labeled cells with collagen IV immunostaining, PFA perfused cerebral cortex tissues that had been labeled with NeuroTrace in vivo after pial surface dye application were cut into 50µm vibratome sections. Sections were mounted on slides in PBS and single NeuroTrace and *PDGFRβcre:Tomato* double labeled pericytes were imaged at high resolution on a confocal microscope. Cell locations within the slice were



mapped and recorded. Tissue sections were then processed for immunohistochemistry as described above. After staining, the sections were remounted, previously imaged cells were relocated, and high resolution confocal images were acquired of the same cell to determine if they were embedded within a dual layer of the basal lamina. This procedure was repeated on 4 brain tissue sections and sequential images from 11 cells were acquired as indicated in the text.

For photooxidation experiments, cerebral cortex tissues labeled with NeuroTrace in vivo after pial surface dye application were cut into 100 $\mu$ m sections. Tissue sections were washed with 0.1M Tris/HCl buffer, then incubated with 2mg/ml DAB in 0.1M Tris buffer (freshly prepared, ice-cold) for 10 min. Photo-bleaching of NeuroTrace labeled region was achieved by using a 100W mercury lamp (488nm) and a 10x (0.25 NA) objective, and lasted for 40–60 min. During the bleaching, ice-cold DAB-solutions were replaced every 10 min. The illumination was stopped when the fluorescence of NeuroTrace had faded completely. After photo-bleaching, the DAB precipitate could be seen with bright field. Then the tissue sections were rinsed with 1x PBS thoroughly and further processed for EM.

### Quantification and statistics

Images were processed and analyzed using ImageJ software. For image deconvolution (Fig. 4, Supplementary Fig. 2) images were deconvolved with Huygens Professional version 16.05 (Scientific Volume Imaging, The Netherlands) using the CMLE algorithm, with SNR: 20 and 40 iterations. Quantification of NeuroTrace labeling and PDGFR $\beta$ -tdTomato cell colocalization in vivo was acquired at 4 locations per animal from 3 animals. Quantification of PDGFR $\beta$  antibody and PDGFR $\beta$ -tdTomato cell co-localization was acquired at 4 locations of the cortex, across 3 brain sections per animal from 3 animals. For spontaneous vasomotion (Fig. 6) a vasomotion index was calculated on vessels with diameters less than 15 $\mu$ m. Briefly, the vasomotion index was defined as the area under the curve for percent spontaneous changes in vessel diameter over 60 second time lapse sequences with a  $\pm$  5% cutoff threshold. Baseline values were determined as the average diameter of all time points for spontaneous diameter changes during each time-lapse sequence. Vessel measurements were derived from the gradient in light intensity (dI/dx) along a designated line selected perpendicular to the single vessels from frame scan images collected at a frequency of 1Hz. The resulting images were thresholded and the width of the vessel was automatically determined using a custom script in ImageJ. For changes in vessel diameter during CCA occlusion single vessel locations were randomly selected from time-lapse sequences and vessel diameters were manually measured before, 5 minutes after the start of the occlusion (designated ‘during’ in Supplementary Fig. 4) and 10 minutes after reperfusion (designated ‘after’ in Supplementary Fig. 4) in ImageJ. Percent changes in vessel diameter were determined for vessels covered by *SMA-mCherry* expressing SMCs and vessels covered by NeuroTrace-labeled pericytes as indicated.

All data were assumed to have a normal distribution for each statistical and all data are displayed as mean  $\pm$  SD in the text and mean  $\pm$  SEM in graphs unless otherwise indicated. No data was excluded from analysis, no randomization was used to assign experimental subjects and experimenter blinding was not necessary. No statistical methods were used for

predetermined sample size determination but our sample sizes are similar to those reported in previous publications<sup>7, 13, 14, 33</sup>. For each experiment at least 3 animals were used with animal and cell numbers indicated in the text. Each representative image was successfully repeated in at least three image locations for each animal with sample sizes (n) designates as single cells followed over multiple days or single animals imaged as indicated in the text and figure legends. To determine statistical significance for cell density quantifications and for vessel diameter changes (Fig. 7–8, Supplementary Fig. 4), unpaired two-tailed student's t tests or two-way ANOVAs with Bonferroni posttests were used as indicated. Statistical analyses were performed with Microsoft Excel and GraphPad Prism. A p value of <0.05 was considered significant. Investigator blinding and animal randomization were not required for these experiments.

## Supplementary Material

Refer to Web version on PubMed Central for supplementary material.

## Acknowledgments

We thank K. Hirschi (Yale University) for sharing *SMA-mCherry* mice, V. Lindner (Maine Medical Center Research Institute) for sharing *PDGFRβcre* mice, and A. Nishiyama (University of Connecticut) for sharing *NG2cre* mice. This work was supported by the following grants from the National Institutes of Health: R21NS087511, R21NS088411, R01NS0889734, R21AG048181 to J.G., and F32NS090820 to R.A.H.

## References

1. Rouget C. Note on the development of the contractile walls of blood vessels. *C R Acad Sci.* 1874
2. Armulik A, Genové G, Betsholtz C. Pericytes: developmental, physiological, and pathological perspectives, problems, and promises. *Dev Cell.* 2011; 21:193–215. [PubMed: 21839917]
3. Iadecola C, Nedergaard M. Glial regulation of the cerebral microvasculature. *Nat Neurosci.* 2007; 10:1369–1376. [PubMed: 17965657]
4. Daneman R, Zhou L, Kebede AA, Barres BA. Pericytes are required for blood-brain barrier integrity during embryogenesis. *Nature.* 2010; 468:562–566. [PubMed: 20944625]
5. Armulik A, et al. Pericytes regulate the blood-brain barrier. *Nature.* 2010; 468:557–561. [PubMed: 20944627]
6. Shih AY, et al. Robust and fragile aspects of cortical blood flow in relation to the underlying angioarchitecture. *Microcirculation.* 2015; 22:204–218. [PubMed: 25705966]
7. Hill RA, et al. Regional blood flow in the normal and ischemic brain is controlled by arteriolar smooth muscle cell contractility and not by capillary pericytes. *Neuron.* 2015; 87:95–110. [PubMed: 26119027]
8. Winkler EA, Bell RD, Zlokovic BV. Central nervous system pericytes in health and disease. *Nat Neurosci.* 2011; 14:1398–1405. [PubMed: 22030551]
9. Iadecola C. Neurovascular regulation in the normal brain and in Alzheimer's disease. *Nat Rev Neurosci.* 2004; 5:347–360. [PubMed: 15100718]
10. Hall CN, et al. Capillary pericytes regulate cerebral blood flow in health and disease. *Nature.* 2014; 508:55–60. [PubMed: 24670647]
11. Fernández-Klett F, Offenhauser N, Dirnagl U, Priller J, Lindauer U. Pericytes in capillaries are contractile in vivo, but arterioles mediate functional hyperemia in the mouse brain. *Proc Natl Acad Sci U S A.* 2010; 107:22290–22295. [PubMed: 21135230]
12. Yemisci M, et al. Pericyte contraction induced by oxidative-nitrative stress impairs capillary reflow despite successful opening of an occluded cerebral artery. *Nat Med.* 2009; 15:1031–1037. [PubMed: 19718040]

13. Hartmann DA, et al. Pericyte structure and distribution in the cerebral cortex revealed by high-resolution imaging of transgenic mice. *Neurophotonics*. 2015; 2:041402. [PubMed: 26158016]
14. Wei HS, et al. Erythrocytes Are Oxygen-Sensing Regulators of the Cerebral Microcirculation. *Neuron*. 2016; 91:851–862. [PubMed: 27499087]
15. Vates GE, Takano T, Zlokovic B, Nedergaard M. Pericyte constriction after stroke: the jury is still out. *Nat Med*. 2010; 16:959. author reply 960. [PubMed: 20823870]
16. Sweeney MD, Ayyadurai S, Zlokovic BV. Pericytes of the neurovascular unit: key functions and signaling pathways. *Nat Neurosci*. 2016; 19:771–783. [PubMed: 27227366]
17. Attwell D, Mishra A, Hall CN, O'Farrell FM, Dalkara T. What is a pericyte? *J Cereb Blood Flow Metab*. 2016; 36:451–455. [PubMed: 26661200]
18. Quinn B, Toga AW, Motamed S, Merlic CA. Fluoro nissl green: a novel fluorescent counterstain for neuroanatomy. *Neurosci Lett*. 1995; 184:169–172. [PubMed: 7715839]
19. Nimmerjahn A, Kirchhoff F, Kerr JND, Helmchen F. Sulforhodamine 101 as a specific marker of astroglia in the neocortex in vivo. *Nat Methods*. 2004; 1:31–37. [PubMed: 15782150]
20. Hill RA, Grutzendler J. In vivo imaging of oligodendrocytes with sulforhodamine 101. *Nat Methods*. 2014; 11:1081–1082. [PubMed: 25357236]
21. Cuttler AS, et al. Characterization of Pdgfrb-Cre transgenic mice reveals reduction of ROSA26 reporter activity in remodeling arteries. *Genesis*. 2011; 49:673–680. [PubMed: 21557454]
22. Zhu X, Bergles DE, Nishiyama A. NG2 cells generate both oligodendrocytes and gray matter astrocytes. *Development*. 2008; 135:145–157. [PubMed: 18045844]
23. Zhu X, et al. Age-dependent fate and lineage restriction of single NG2 cells. *Development*. 2011; 138:745–753. [PubMed: 21266410]
24. Meisslitzer-Ruppitsch C, Röhrl C, Neumüller J, Pavelka M, Ellinger A. Photooxidation technology for correlated light and electron microscopy. *J Microsc*. 2009; 235:322–335. [PubMed: 19754726]
25. Meiblitzer-Ruppitsch C, et al. Electron microscopic visualization of fluorescent signals in cellular compartments and organelles by means of DAB-photoconversion. *Histochem Cell Biol*. 2008; 130:407–419. [PubMed: 18463889]
26. Morris AWJ, et al. Vascular basement membranes as pathways for the passage of fluid into and out of the brain. *Acta Neuropathol*. 2016; 131:725–736. [PubMed: 26975356]
27. Armstrong JJ, Larina IV, Dickinson ME, Zimmer WE, Hirschi KK. Characterization of bacterial artificial chromosome transgenic mice expressing mCherry fluorescent protein substituted for the murine smooth muscle alpha-actin gene. *Genesis*. 2010; 48:457–463. [PubMed: 20506352]
28. Shen Z, Lu Z, Chhatbar PY, O'Herron P, Kara P. An artery-specific fluorescent dye for studying neurovascular coupling. *Nat Methods*. 2012; 9:273–276. [PubMed: 22266543]
29. Harb R, Whiteus C, Freitas C, Grutzendler J. In vivo imaging of cerebral microvascular plasticity from birth to death. *J Cereb Blood Flow Metab*. 2013; 33:146–156. [PubMed: 23093067]
30. Gerhardt H, Betsholtz C. Endothelial-pericyte interactions in angiogenesis. *Cell Tissue Res*. 2003; 314:15–23. [PubMed: 12883993]
31. Hughes S, Chan-Ling T. Characterization of smooth muscle cell and pericyte differentiation in the rat retina in vivo. *Invest Ophthalmol Vis Sci*. 2004; 45:2795–2806. [PubMed: 15277506]
32. Murphy TH, Li P, Betts K, Liu R. Two-photon imaging of stroke onset in vivo reveals that NMDA-receptor independent ischemic depolarization is the major cause of rapid reversible damage to dendrites and spines. *J Neurosci*. 2008; 28:1756–1772. [PubMed: 18272696]
33. Drew PJ, Shih AY, Kleinfeld D. Fluctuating and sensory-induced vasodynamics in rodent cortex extend arteriole capacity. *Proc Natl Acad Sci U S A*. 2011; 108:8473–8478. [PubMed: 21536897]
34. Simard M, Arcuino G, Takano T, Liu QS, Nedergaard M. Signaling at the gliovascular interface. *J Neurosci*. 2003; 23:9254–9262. [PubMed: 14534260]
35. Borysova L, Wray S, Eisner DA, Burdyga T. How calcium signals in myocytes and pericytes are integrated across in situ microvascular networks and control microvascular tone. *Cell Calcium*. 2013; 54:163–174. [PubMed: 23867002]
36. Cuevas P, et al. Pericyte endothelial gap junctions in human cerebral capillaries. *Anat Embryol*. 1984; 170:155–159. [PubMed: 6517350]

37. Bell RD, et al. Pericytes control key neurovascular functions and neuronal phenotype in the adult brain and during brain aging. *Neuron*. 2010; 68:409–427. [PubMed: 21040844]
38. Madisen L, et al. A robust and high-throughput Cre reporting and characterization system for the whole mouse brain. *Nat Neurosci*. 2010; 13:133–140. [PubMed: 20023653]
39. Oakley H, et al. Intraneuronal beta-amyloid aggregates, neurodegeneration, and neuron loss in transgenic mice with five familial Alzheimer’s disease mutations: potential factors in amyloid plaque formation. *J Neurosci*. 2006; 26:10129–10140. [PubMed: 17021169]
40. Holtmaat A, et al. Long-term, high-resolution imaging in the mouse neocortex through a chronic cranial window. *Nat Protoc*. 2009; 4:1128–1144. [PubMed: 19617885]
41. Whiteus C, Freitas C, Grutzendler J. Perturbed neural activity disrupts cerebral angiogenesis during a postnatal critical period. *Nature*. 2014; 505:407–411. [PubMed: 24305053]
42. Sano H, et al. Study on PDGF receptor beta pathway in glomerular formation in neonate mice. *Ann N Y Acad Sci*. 2001; 947:303–305. [PubMed: 11795278]
43. Hill RA, Natsume R, Sakimura K, Nishiyama A. NG2 cells are uniformly distributed and NG2 is not required for barrel formation in the somatosensory cortex. *Mol Cell Neurosci*. 2011; 46:689–698. [PubMed: 21292011]

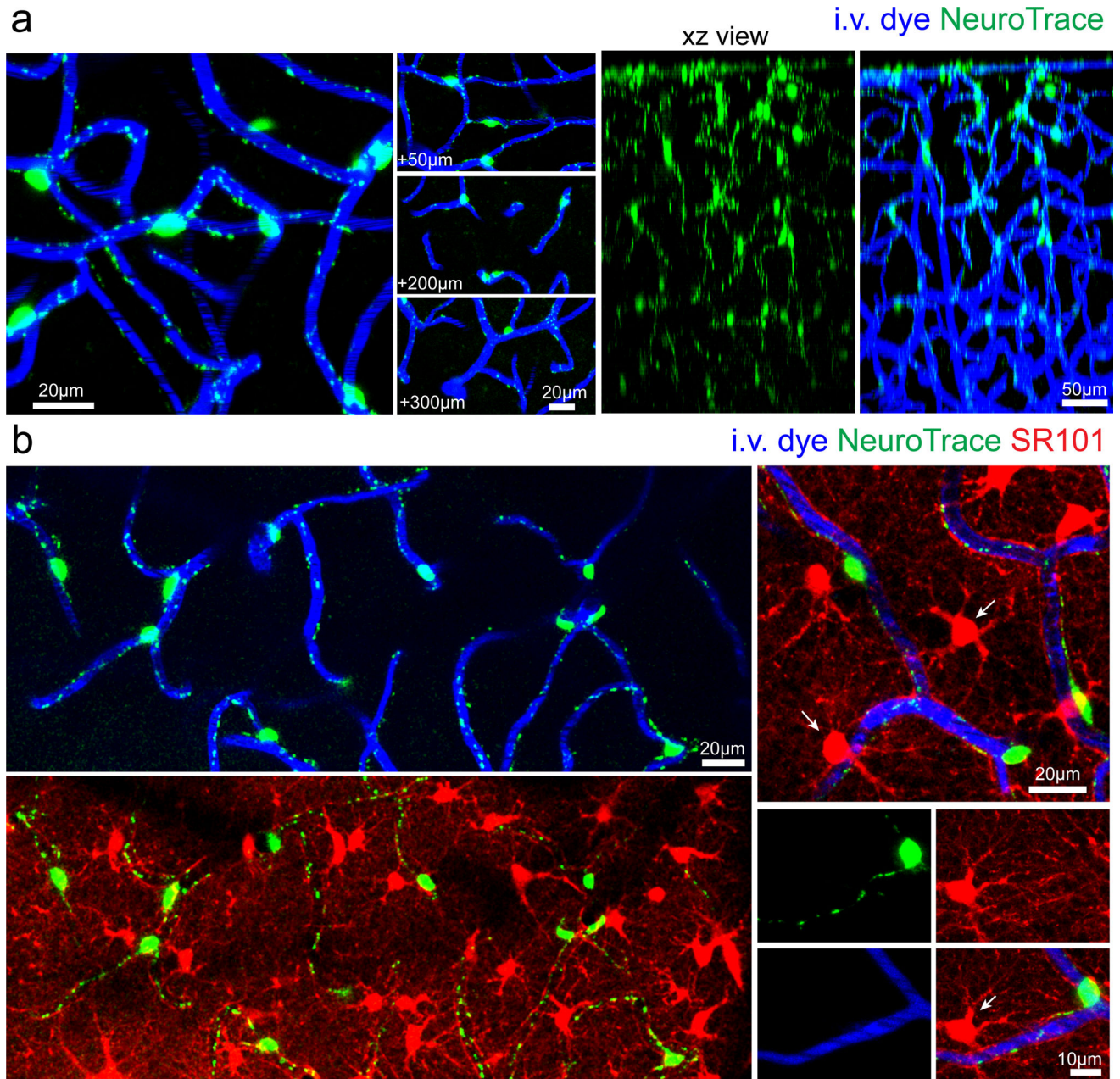


**Figure 1. NeuroTrace labels vascular cells lining capillaries in the live mouse brain**  
**(a)** *In vivo* images captured from the cerebral cortex of a wildtype mouse after topical application of the fluoro-nissl derivative NeuroTrace 500/525 showing exclusive pericyte labeling and labeling at various depths from the cortical pial surface. **(b)** *In vivo* images showing no overlap between NeuroTrace labeled pericytes and SR101-labeled astrocytes and oligodendrocytes (arrows). Each representative image was successfully repeated in at least three image locations in at least three animals.

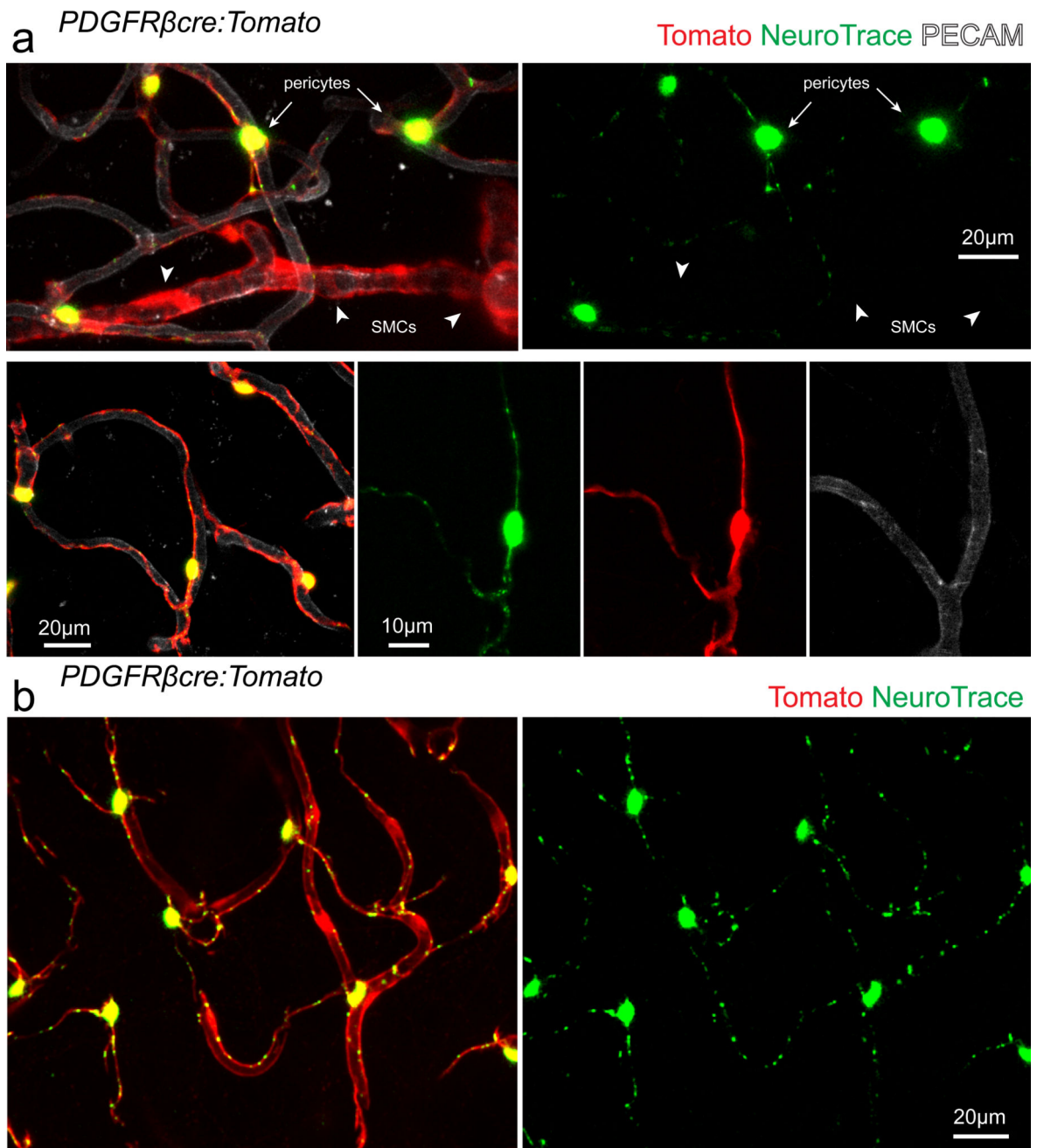


**Figure 2. NeuroTrace exclusively labels PDGFR $\beta$  expressing capillary pericytes (a–b)** *In vivo* images captured from *PDGFR $\beta$ cre:Tomato* transgenic mice injected with fluorescent conjugated PECAM antibody showing complete and exclusive labeling of fusiform capillary pericytes (arrows) but not SMCs with circumferential morphology (arrowheads) with NeuroTrace dye. Each representative image was successfully repeated in at least three image locations in at least three animals.

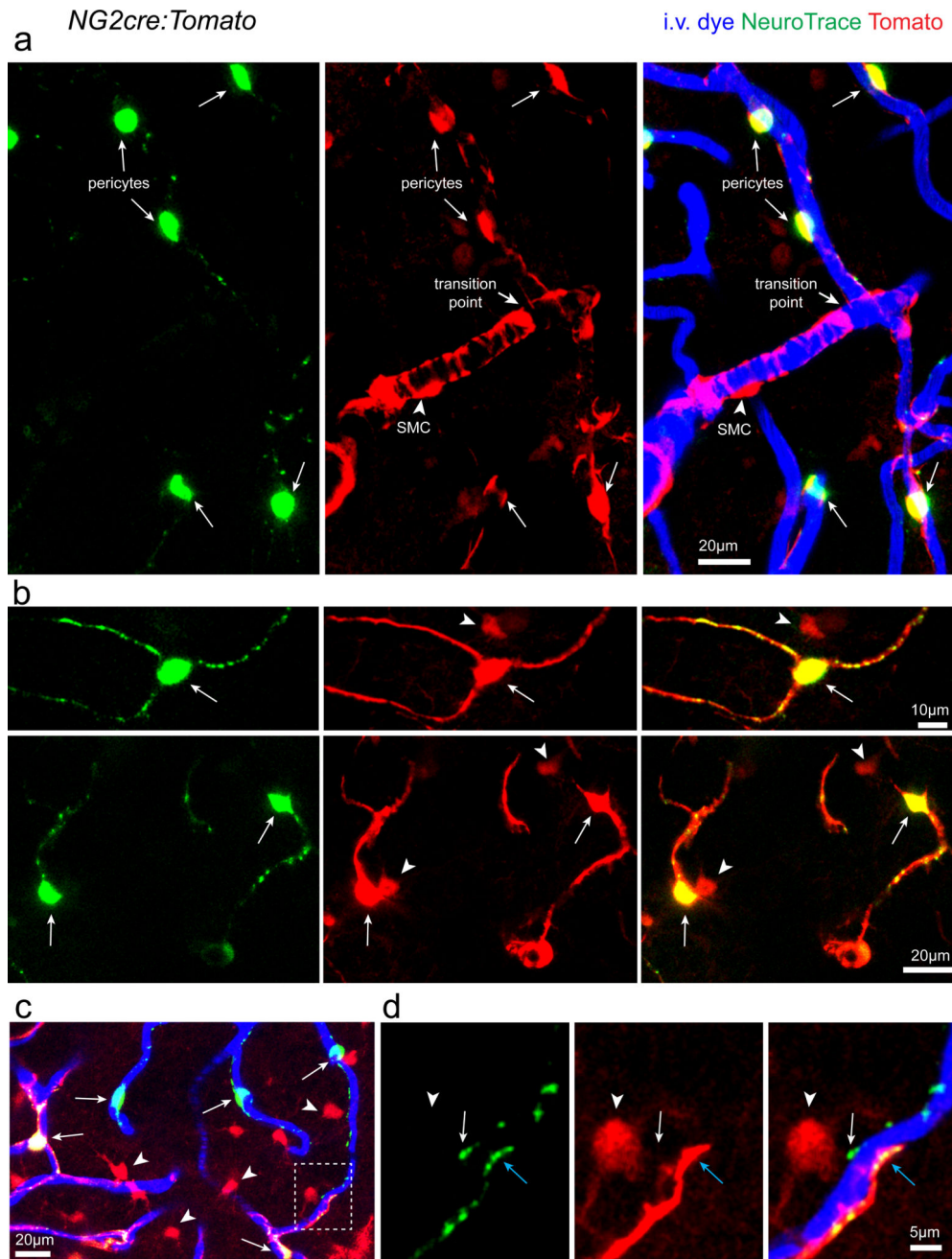


**Figure 3. NeuroTrace labels capillary pericytes and not arteriolar smooth muscle cells**  
**(a)** In vivo images captured from *NG2cre:Tomato* transgenic mice showing complete labeling of fusiform capillary pericytes (arrows) but not SMCs with circumferential morphology (arrowheads), NG2-glia, or oligodendrocytes all of which are also labeled with Tomato in *NG2cre* mice. **(b)** High resolution images of single NeuroTrace labeled pericytes (arrows) in *NG2cre:Tomato* mice with oligodendrocyte lineage cells also labeled with the Tomato reporter (arrowheads). **(c–d)** Low and high zoom in vivo images demonstrating that NeuroTrace labels all pericytes (arrows) unlike *NG2cre* reporter mice due to incomplete cre recombination. Zoomed image shows the transition from transgenic Tomato reporter labeled

pericytes (blue arrows) to non-labeled cells with NeuroTrace labeling in all pericytes (arrows). Parenchymal oligodendrocyte lineage cells are also labeled with Tomato reporter (arrowheads). Each representative image was successfully repeated in at least three image locations in at least three animals.

Author Manuscript

Author Manuscript

Author Manuscript

Author Manuscript



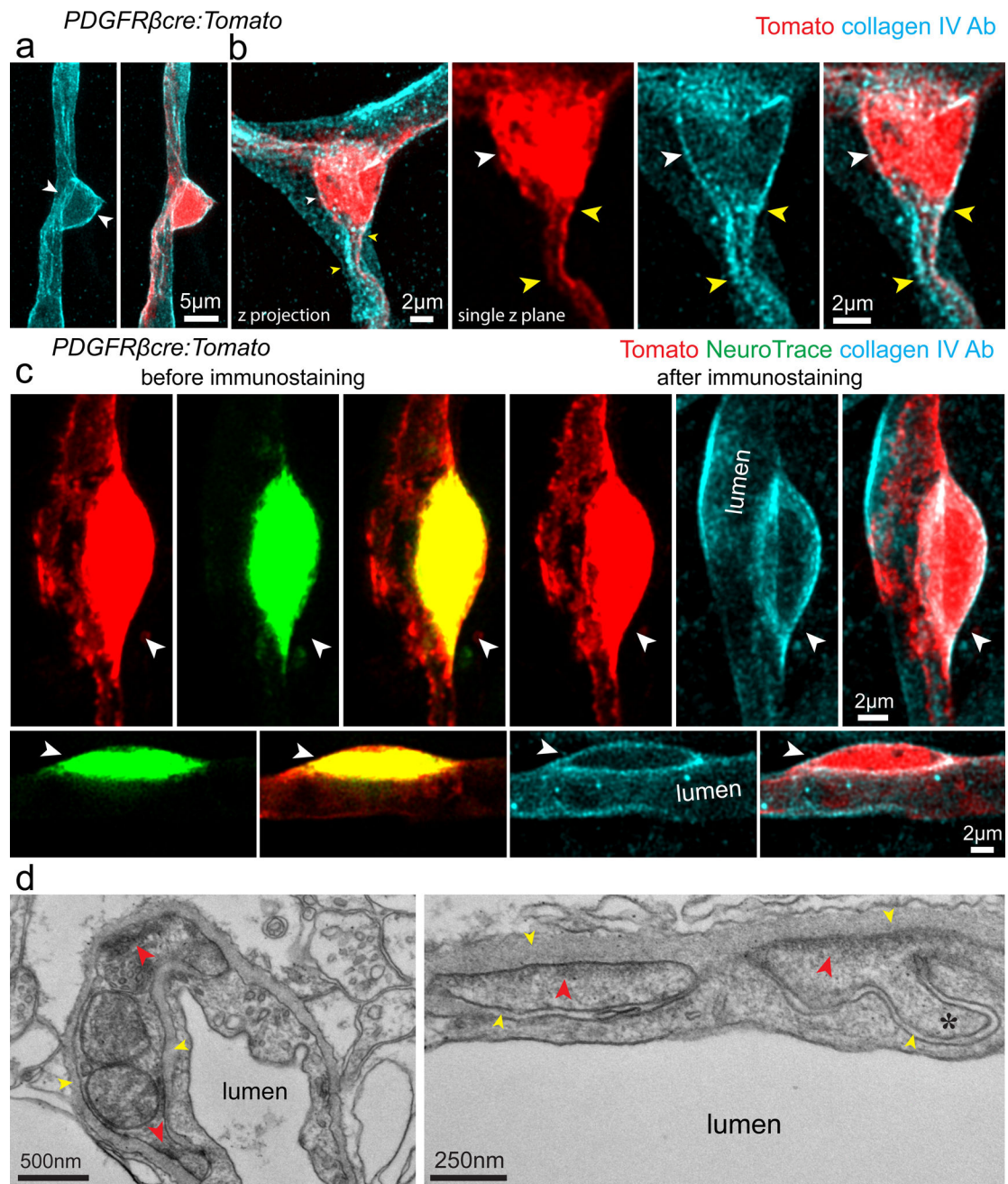


**Figure 4. NeuroTrace-labeled pericytes are embedded within the basal lamina**

(a) Confocal fluorescence image captured from the cortex of a *PDGFRβcre:Tomato* transgenic mouse stained with collagen IV antibody showing detection of the double layer of the basal lamina (arrows) completely surrounding a capillary pericyte labeled with Tomato. (b) Confocal projection (left) and single z plane (right) of a single pericyte cell body (white arrowheads) and proximal processes (yellow arrowheads) showing complete envelopment within the collagen IV labeled basal lamina layers. (c) Images of single pericytes (arrowheads) labeled with NeuroTrace and Tomato and then reimaged after immunostaining for collagen IV further confirming that NeuroTrace labels capillary pericytes (n=11 cells)

**(d)** Transmission electron micrographs taken from tissue that has undergone photooxidation of NeuroTrace labeled pericytes for detection of diaminobenzidine (DAB) electron dense products. Red arrowheads indicate potential photooxidized DAB products found within the pericyte cell body and processes. Yellow arrowheads indicated double basal lamina surrounding the pericytes. Asterisk indicates likely “peg and socket” pericyte process. Each representative image was successfully repeated in at least three image locations in at least three animals.

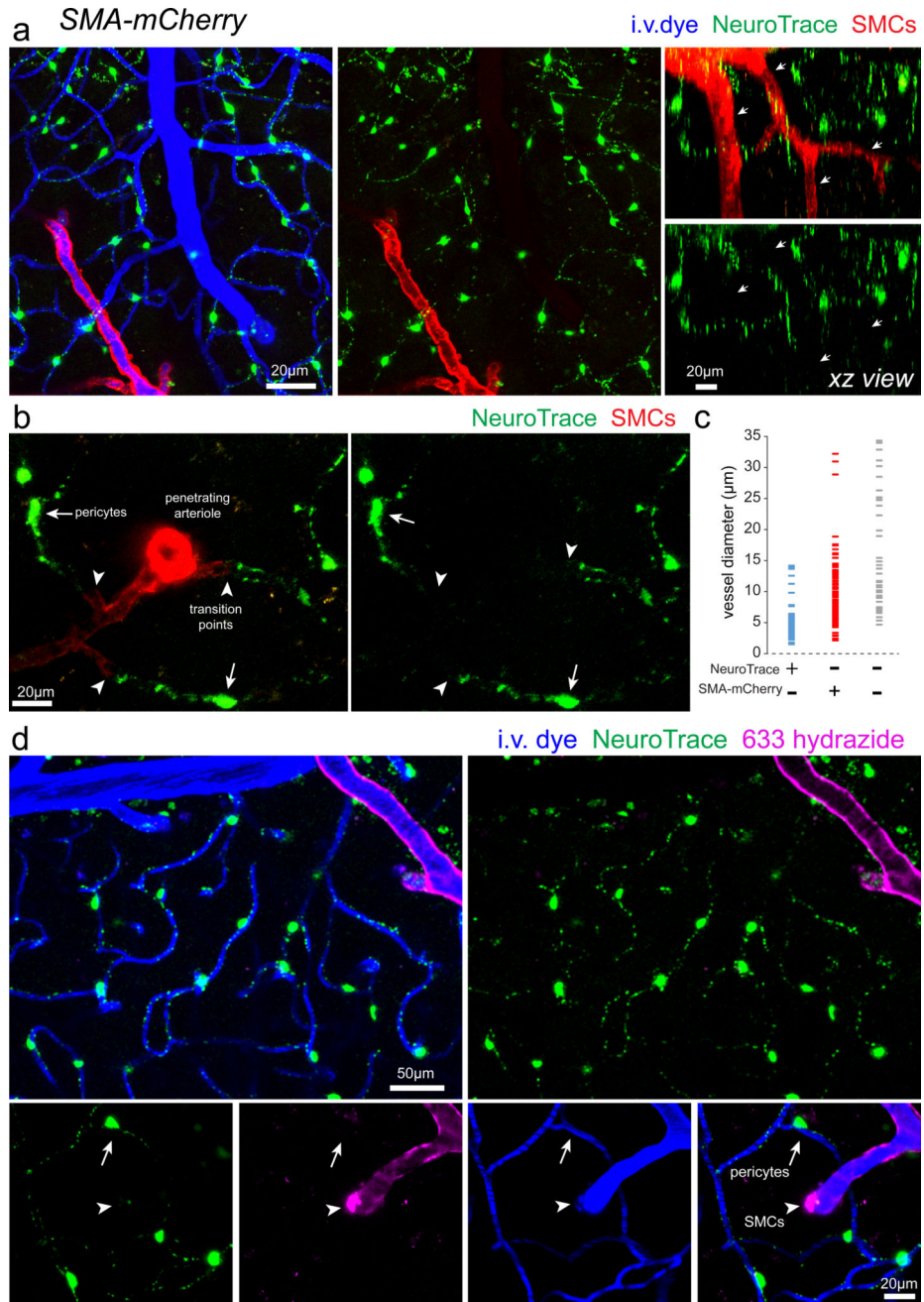


**Figure 5. NeuroTrace does not label  $\alpha$ -smooth muscle actin expressing mural cells (a–b)** In vivo images captured from the cortex of a transgenic mouse with mCherry fluorescent protein specifically in smooth muscle actin (SMA) expressing smooth muscle cells (SMCs) (*SMA-mCherry*) labeled with NeuroTrace. No co-labeling was detected between mCherry and NeuroTrace demonstrating that smooth muscle cells do not take up this dye (arrowheads). **(c)** Distribution of vessel diameters for vessels covered by NeuroTrace-labeled cells, *SMA-mCherry*-labeled cells, or neither. **(d)** In vivo images showing labeling with the arteriole specific fluorescent dye 633 hydrazide (arrowheads) and no co-labeling on vessels covered by NeuroTrace-labeled pericytes (arrows). Each

representative image was successfully repeated in at least three image locations in at least three animals.

Author Manuscript

Author Manuscript

Author Manuscript

Author Manuscript

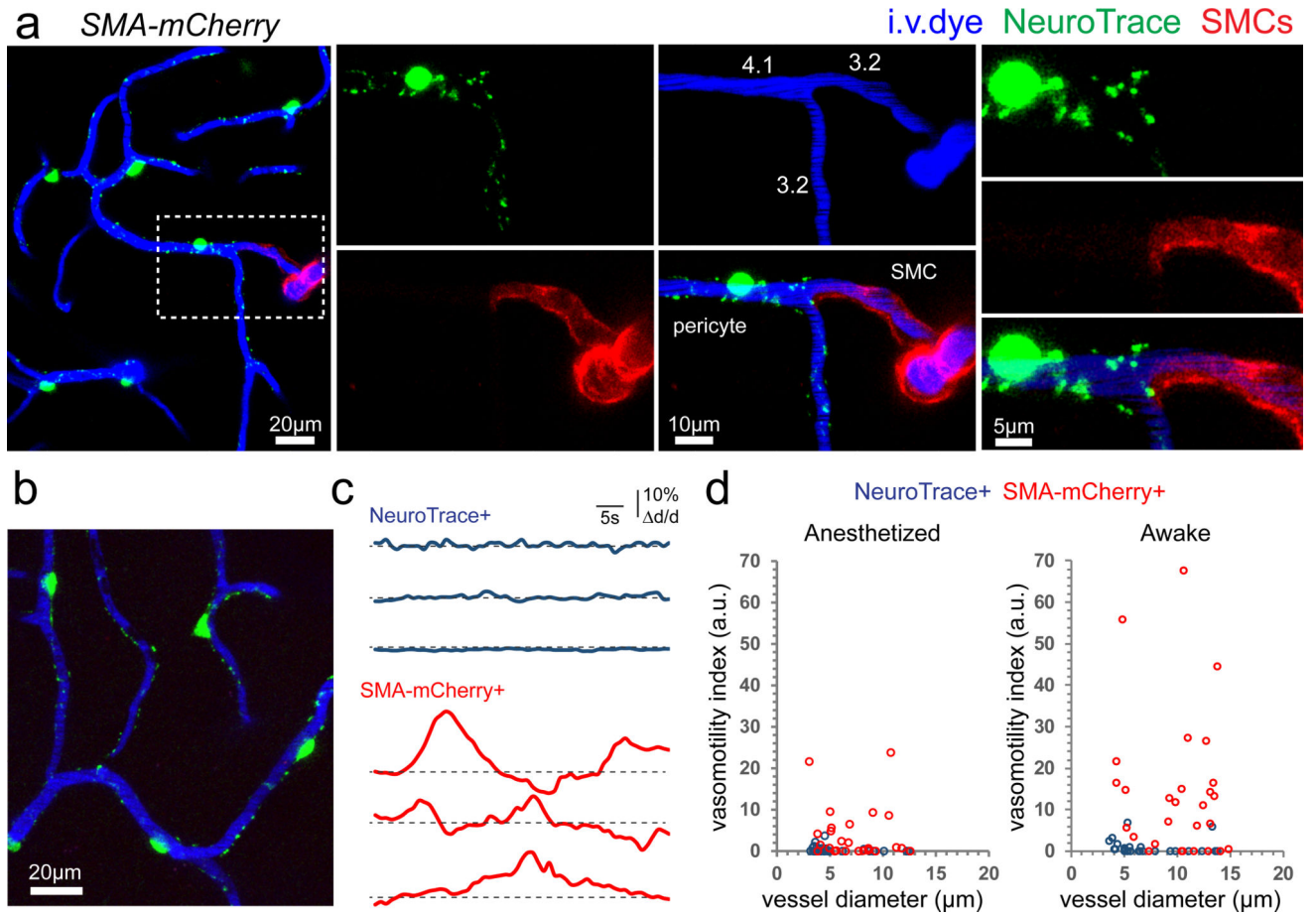


**Figure 6. NeuroTrace-labeled pericytes do not exhibit spontaneous vasomotion**

(a) Terminal smooth muscle actin expressing SMCs in *SMA-mCherry* transgenic mice do not take up NeuroTrace demonstrated by the sharp delineation of mCherry and NeuroTrace labeling (vessel diameters indicated). (b) Distinct morphology of NeuroTrace labeled pericytes in the capillary bed downstream from *SMA-mCherry* expressing cells. (c) Spontaneous diameter changes of three different NeuroTrace-covered or *SMA-mCherry* covered vessels acquired in vivo from awake head fixed mice. (d) The relationship between vessel diameter and vasomotility index in anesthetized and awake animals for vessels covered by NeuroTrace labeled pericytes or *SMA-mCherry* labeled SMCs (Anesthetized: NeuroTrace-labeled 31 vessels, *SMA-mCherry* labeled 30 vessels from n=5 mice; Awake: NeuroTrace-labeled 26 vessels, *SMA-mCherry* labeled 28 vessels, from n=4 mice). Each representative image was successfully repeated in at least three image locations in at least three animals.

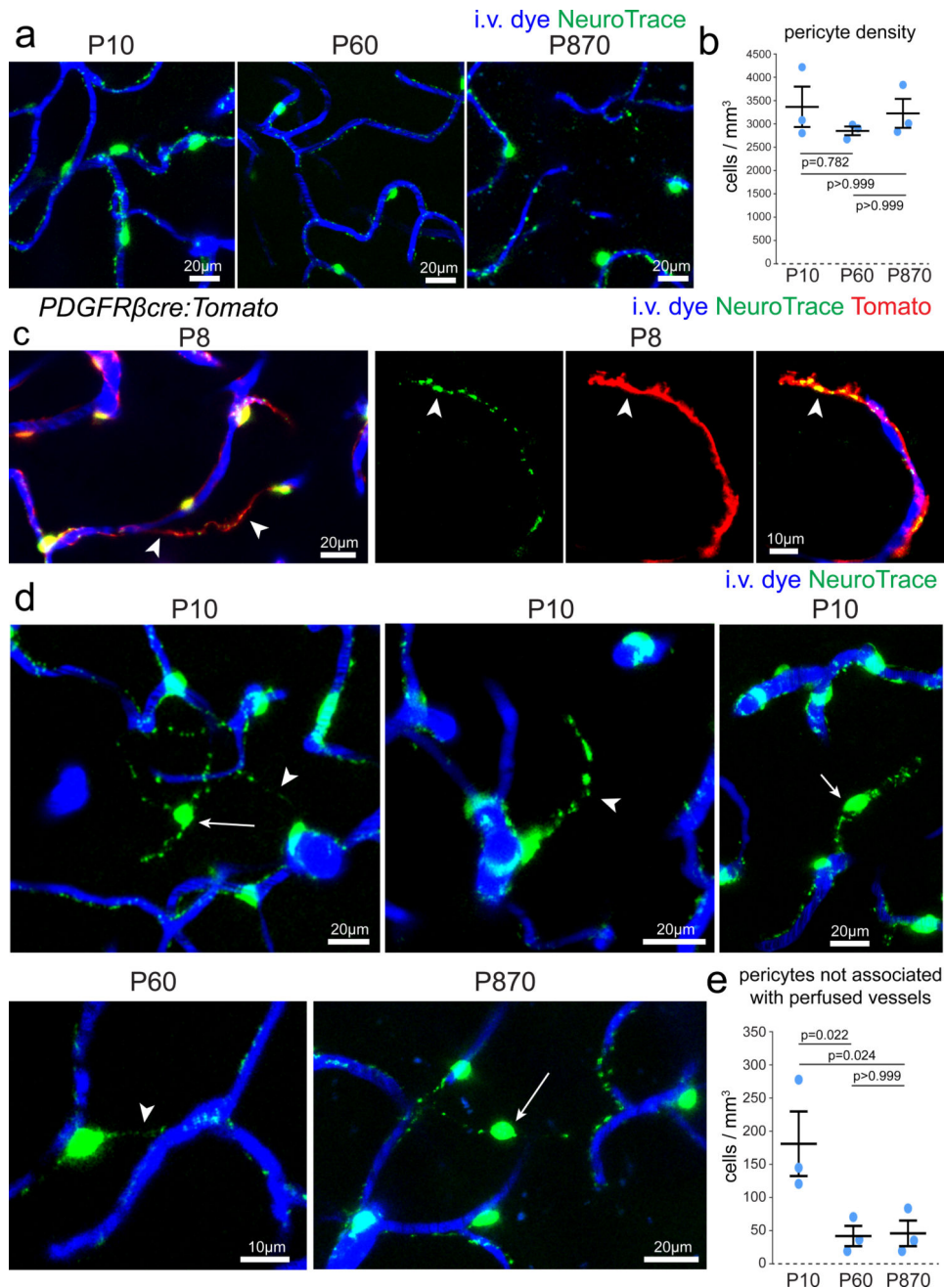


**Figure 7. In vivo imaging of pericytes during development into advanced aging**  
**(a–b)** NeuroTrace labeling and pericyte distribution at postnatal (P) days 10, 60 and 870 showing no significant differences in pericyte labeling or number ( $n=3$  mice per group, mean  $\pm$  SEM, two-way ANOVA Bonferroni posttest  $p$  value as indicated P10 vs. P60  $t=1.309$   $df=4$ , P10 vs. P870  $t=0.3553$   $df=4$ , P60 vs. P870  $t=0.9542$   $df=4$ ). **(c)** In vivo images of captured from P8 *PDGFRβcre:Tomato* transgenic mice showing Tomato and NeuroTrace labeled pericyte processes not associated with perfused vessels (arrowheads). **(d)** In vivo images captured from P10, P60 and P870 mice showing pericytes not associated with perfused vessels at all ages **(e)** The prevalence of pericytes not associated with perfused

vessels declines with age (n=3 mice per group, mean  $\pm$  SEM, two-way ANOVA Bonferroni posttest p value as indicated P10 vs. P60  $t=5.047$   $df=4$ , P10 vs. P870  $t=4.9$   $df=4$ , P60 vs. P870  $t=0.147$   $df=4$ ). Each representative image was successfully repeated in at least three image locations in at least three animals.

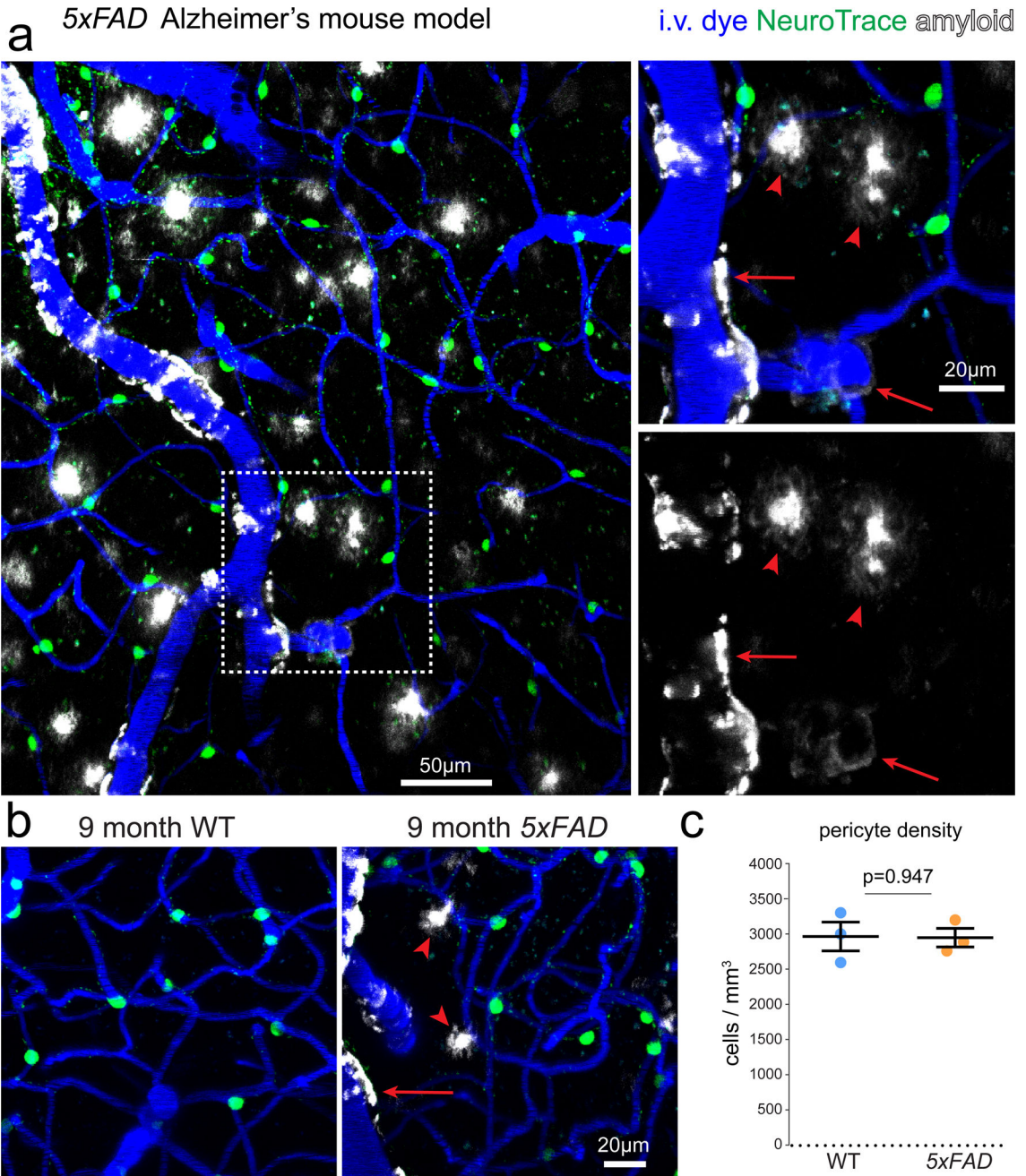


**Figure 8. Pericyte imaging in Alzheimer's mouse models in vivo**  
**(a)** Pericyte labeling in a mouse model of Alzheimer's disease (5x*FAD*) showing cerebral amyloid angiopathy on arterioles and precapillary arterioles (arrows) but not pericyte-covered capillaries. Arrowheads indicate amyloid plaques found throughout the parenchyma.  
**(b)** In vivo images captured from the cortex of aged matched wild type and 5x*FAD* mice. Arrows indicate cerebral amyloid angiopathy and arrowheads indicate amyloid plaques.  
**(c)** Pericyte labeling density is not different between age-matched wildtype and 5x*FAD* transgenic mice. (n=3 mice per group, mean ± SEM, unpaired two-tailed student's t-test p



value as indicated,  $t=0.07051445$   $df=4$ ). Each representative image was successfully repeated in at least three image locations in at least three animals.

Author Manuscript

Author Manuscript

Author Manuscript

Author Manuscript